Jül-Conf-45 D2-2

ICANS V

MEETING OF THE INTERNATIONAL COLLABORATION ON
ADVANCED NEUTRON SOURCES

June 22-26, 1981

Preliminary Neutronics of a Reflected 'T'-Shape Premoderator/Moderator for the Weapons Neutron Research Facility

G. J. Russell, M. M. Meier, and H. Robinson
Los Alamos National Laboratory
Los Alamos, New Mexico 87545, U.S.A.

A. D. Taylor
Rutherford and Appleton Laboratories
Chilton, Didcot, OXON OX11 0QX, U.K.

ABSTRACT

At the Los Alamos pulsed spallation neutron source, we are developing the capability of measuring absolute neutron spectra and beam fluxes $\lesssim 10$ eV and neutron pulse widths $\lesssim 0.2$ eV. We utilize this capability in a development program directed toward characterizing and optimizing our source and providing basic neutronics data relevant to spallation neutron sources. We describe here the facilities being developed and show some preliminary results.

INTRODUCTION

The Weapons Neutron Research facility (WNR) is an operational pulsed spallation neutron source[1] at the Los Alamos National Laboratory. The layout of the WNR is illustrated in Fig. 1. The 800-MeV proton source for the WNR is the Clinton P. Anderson Meson Physics Facility (LAMPF).[2] Note in Fig. 1 that the WNR has two target areas: a) a high-current target area shielded to accept 20 μA, and b) a low-current target area shielded to accept 0.1 μA. The high-current target is equipped with a flexible target-moderator-reflector handling system which allows us to relatively easily interchange targets and moderators for various experimental programs. We use the high-current target area to provide neutrons for nuclear physics applications ($\sim$1 eV to $\sim$300 MeV) and for materials science research ($\lesssim$1 eV). We use the low-current target area to study (and optimize) the neutronics of moderated neutrons.

The characteristics of the WNR proton beam, and the capabilities built into the low-current target area are unique in the world; they include:

- continuously variable proton pulse widths from $\sim$35 ns to $\sim$8.5 μs,
- variable proton pulse repetition rates from 1 Hz to 120 Hz,
- a shielded (vertical) flight path for measuring absolute neutron beam fluxes and spectra $\lesssim$10 eV, and
- a time-analyzer arm (attached to the vertical flight path) for measuring neutron pulse widths from moderators.

Also, the low-current target area is readily accessible for moderator, collimator, and detector alignment, and for changing target-moderator-reflector configurations.

Once we have studied, optimized, and characterized the neutronic performance of a particular target-moderator-reflector geometry, we can incorporate the changes into the high-current target to take advantage of the neutron enhancement. We recently demonstrated this capability by measuring (in the low-current target area) an increase in neutron beam fluxes ($\lesssim$0.5 eV) of $\sim$1.7 when changing the poison between our premoderator and moderator from 0.076-cm of Cd to 0.0025-cm of Gd. We made the poison change in the high-current target during the next LAMPF cycle break. Subsequent neutron scattering measurements in the high-current target area confirmed our predicted neutronic enhancement.

The combination of the WNR low- and high-current target areas, the facilities built into each area, continuously variable proton pulse widths, and variable proton repetition rates provide us with an unequaled

capability to characterize the neutronics of spallation neutron sources using 800-MeV protons. Our spallation target-moderator-reflector development program has been described in Refs. 3 and 4, and is summarized in Table I.

We describe here the capabilities built into the WNR low-current target area for neutronics measurements $\lesssim 10$ eV, and show some preliminary results. We use calculated predictions from Monte Carlo codes to help guide our experimental program. Our measurement program also provides a check on the validity of the computer codes (model evaluation). The computer codes used are: a) the Oak Ridge National Laboratory code HETC for particle transport $\gtrsim 20$ MeV,[5] b) the Los Alamos code MCNP for neutron and gamma-ray transport $\lesssim 20$ MeV,[6] and c) the Ispera code TIMOC implemented at the Rutherford Laboratory.[7,8]

WNR LOW-CURRENT TARGET FACILITIES

The WNR low-current target area is built of reinforced concrete (0.2-m thick), and shielded with ~ 4.9-m dirt. The center portion of the floor (~ 30 m^2) is aluminum; the walls are ~ 6.2 m from the center of the room to minimize neutron return from the walls to configurations located at room-center. In Fig. 2, we show the location of the vertical flight path in the low-current target area. The details of this flight path are illustrated in Figs. 3-5. The nominal distance from the proton beam line to the center of the BF_3 neutron detector is ~ 5.61 m; the nominal distance from the diffraction crystal to the ^{3}He detector is ~ 1.02 m.

The shielding in the vertical flight path and that around the time-analyzer arm is sufficient to make background corrections to the data small. Specifically, the shielding in the vertical flight path consists of the following materials: a) 0.89-m iron, b) ~ 3.3-m iron shot, c) ~ 0.90-m lead shot, d) 7.6-cm borated (5 wt%) polyethylene, and e) 2.5-cm borated (32 wt%) polyethylene. The detector/crystal chamber (at the bottom of the flight path) is lined with 0.051-cm-thick cadmium. On the side opposite the time-analyzer arm, the detector/crystal chamber is shielded by ~ 10-cm paraffin and ~ 14-cm iron shot. The neutron shield around the time-analyzer arm consists of the following materials: a) 36-cm iron, b) ~ 50-cm paraffin, c) 5.1-cm borated (both 5 wt% and 32 wt%) polyethylene, d) 0.79-cm boral, and e) 0.076-cm cadmium. In the vertical flight path, we initially shape the neutron beam with two 5.1-cm-thick borated (32 wt%) polyethylene collimators. These two collimators are located at 3.96 m and 0.24 m from the center of the BF_3 detector. A final collimator (located 2.5 cm from the center of the BF_3 detector) is a 1.8-cm-thick piece of sintered natural boron carbide; the 2.0 cm by 2.0-cm hole through the boron carbide collimator is lined with 0.0025-cm gadolinium. There are additional baffles (to reduce the penumbra in the moderator field-of-view) located between the aluminum floor and the target-moderator-reflector configuration; these baffles are made from 2.5-cm-thick borated (32 wt%) polyethylene. The need for additional baffles and selected shielding is being evaluated.

A Pyrolitic Graphite (PG) crystal with a 0.4° mosaic (FWHM) was used in our initial neutron pulse width measurements. The crystal was set in as backscattering a geometry as practical (a 2ϑ of 137°) to minimize the $\cot\vartheta\,\Delta\vartheta$ contribution to the resolution. We plan to use crystals with smaller d-spacings in the time-analyzer arm which will enable us to measure neutron pulse widths at higher energies than available with the PG crystal.

THE 'T'-SHAPE PREMODERATOR/MODERATOR

An unreflected 'T'-shape premoderator/moderator is illustrated in Fig. 6. Such a target-moderator configuration has good neutronic coupling (useful-neutrons/protons•sr). Note in Fig. 6, that both center and offset moderator geometries can be accommodated with the larger leg of the 'T'; offset geometry is indicated. We are using a premoderator/moderator approach where the premoderator and moderator may be different materials. The choice of materials will be based on neutronic performance (intensity and pulse width), beam quality (contamination of the useful neutron beam by charged particles, gamma-rays, and high-energy neutrons), and radiation damage considerations.

For pulsed spallation neutron sources, a neutron reflector can enhance the thermal neutron production by factors of 2-4. [3,9] A reflected 'T'-shape premoderator/moderator is illustrated in Figs. 7 and 8. We are presently concentrating our efforts on studying the neutronics of 'T'-shape premoderator/moderators, and have installed a prototype reflected 'T'-shape premoderator/moderator in the high-current target area. An optimized version of this configuration (using ambient temperature moderators) will be installed in the high-current target area early in 1982.

Our interest in the 'T'-shape configuration is best illustrated using Fig. 9. In this figure, we depict the layout of the neutron flight paths in the high-current target area. The flight paths occur in clusters of three at right angles to each other. Our goal is to provide optimized neutron beams to as many flight paths as possible so that concurrent experiments can be performed. One orientation of the 'T'-shape moderator relative to these flight paths is shown in Fig. 10. The premoderator/moderator approach allows individual moderators to be optimized for a particular class of instruments using the neutron beams (see Fig. 11).

DETECTORS AND ELECTRONICS

In the vertical flight path, we use a 2.54-cm-diam BF_3 proportional counter to detect moderated neutrons ($\lesssim$10 eV). The counter is oriented with its axis perpendicular to the neutron beam; its sensitive area is

defined by a slot (2.5-cm long and exposing half the detector diameter) cut into the 0.076-cm-thick Cd sheath surrounding the detector. The BF_3 pressure is 40-cm Hg and the boron is enriched to 96% ^{10}B. For 0.025-eV neutrons, the detector efficiency, averaged over the effective area of the neutron beam, is 0.101. Commercial bias supplies, preamplifiers, amplifiers, and integral discriminators are used in a conventional manner to generate timing pulses for events occuring in the counter. We set the discriminator bias at 42% of the $^{10}B(n,\alpha)^7Li^*(0.478\ MeV)$ peak pulse level, a level at which 10.0% of the total (n,α) events are rejected. Following a 50 μs delay after the proton burst strikes the target, the data are electronically gated 'on' during an 8 or 12 ms period depending on the effective LAMPF repetition rate. The former is done to reject the extremely high counting rates at early times, and the latter to eliminate frame overlap.

A capacitive pickup located in the WNR beam line senses the proton pulse 80 ns before it strikes the spallation target. This pulse starts a clock which can accept multiple stops from the neutron detector. The conversion cycle (70 ns), detector resolution, cable delay differences and time slewing in the discriminators are negligible relative to the 3.2 μs channel width of the clock. The digitized times are internally stored in a 16-word buffer which derandomizes the acquisition rate. The clock/buffer is interfaced to the computer through CAMAC. Data are transferred via a direct memory access (DMA) channel to a set of three 256 word buffers in main memory. When one of these buffers fills, a histogramming task is activated which increments the buffer relative addresses in a data area. Simultaneously, DMA storage into the computer is switched to a new buffer. The system was tested with random stops at a continuous rate of 55 kHz at which the clock buffer began to completely fill. At a 50 kHz rate, deadtime measurements were made and found to be less than 0.01%. In general, maximum instantaneous rates from the BF_3 counter were less than 8 kHz and electronic dead times were ignored.

At high instantaneous rates, the BF_3 detector incompletely collects the charge generated by each event. This effectively reduces the detector gain and efficiency. One can study this effect by obtaining neutron time-of-flight data at short proton bursts (where the rates are low enough that the effect is negligible) and with longer proton pulses. The spectrum of the ratio of these spectra should be flat where the effect is negligible; however, as the pulse width is increased, the relative efficiency in the high-rate portion of the Maxwellian region of the neutron spectrum decreases. Such a study was performed and the data are shown in Fig. 12. These effects are negligible for our rates and were ignored.

The BF_3 detector must also recover from the very high counting rates occuring shortly after the protons strike the target. One can follow a procedure similar to that described in the preceeding paragraph, that is, taking the ratio of the counting rate near the fast-burst to that in the Maxwellian as a function of proton pulse width. By observing the behavior of a time region as a function of pulse width, one can extrapolate to zero pulse-width to estimate the necessary correction for that region. For the neutron spectra reported here, we estimate $< 2\%$

losses for neutron energies < 4 eV. We have not made this correction to the data.

In the time-analyzer arm, a single 1.27-cm-diam ^{3}He counter (at 10 atm) is used to detect neutrons. The diameter of this detector closely matches the neutron beam spread from the moderator surface and the mosaic of the PG crystal.

PROTON MONITORING

As part of the WNR target-moderator-reflector development program, absolute measurements of neutron beam fluxes and spectra are planned. Aluminum foils are presently used to obtain the number of protons striking a target, and an 'on-line' proton monitoring system based on secondary emission monitors (SEM's) is being implemented.[10] Two SEM's (one with an Au-plated emitter and one with an Al emitter) have been installed in the low-current target beam line; these SEM's are ~ 1 m upstream of the neutron producing target. Although a failure in our charge integration electronics precluded our use of the system as an absolute proton monitor, the following conclusions are valid: a) the SEM's are stable (relative to neutron production) to ± 0.9% over a ten-day interval, and b) the linearity of the SEM's (again referenced to neutron production) was better than ± 0.9% (1 σ) over the proton pulse width range 35 ns to 2.0 μs. With a reconfiguration of electronics, we expect to use SEM's (in conjunction with periodic Al foil activations) as an absolute monitor of proton charge striking a target.

DATA REDUCTION AND ANALYSIS

We want to measure 'useful' neutrons, that is, neutrons of a given energy which originate in the moderator and reach the detector by a direct route through the collimated flight path. All other neutrons arriving at the detector are classed as 'background'. We estimate this background component by measuring the detector response when the useful neutron beam is attenuated by a 1.8-cm-thick sintered B_4C filter. We placed this filter as close to the moderator surface as practical (~1.2 m). At ~600 eV, this filter has an attenuation of 1/e; at 10 eV, the attenuation is ~0.04%. With the filter in place, neutrons detected below ~10 eV arise from the moderation of fast neutrons in the collimators and from neutrons reaching the detector by non-direct paths. To get the sub-cadmium neutron spectrum from a moderator, we estimate the neutron background component by measuring the detector response when the useful neutron beam is attenuated by a 0.076-cm-thick Cd sheet.

Raw spectral distributions are measured by time-of-flight (TOF) techniques over the 5.61 -m vertical flight path, and are binned into 3.2-μs time channels. Using SEM values for the number of incident protons, signal and background data sets are normalized to each other prior to a point-by-point subtraction. A TOF spectrum, n(t) is

transformed to an energy spectrum, n(E), by the following relationship:

$$n(E) = n(t) \frac{dt}{dE} \qquad (1)$$

Corrections are made to the data for detector efficiency, η_d, for transmission losses through the detector wall, t_w, and for transmission losses through air, t_a, due to absorption and scattering in the 1.56 m of unevacuated flight path at the mean for Los Alamos pressure of 580-mm Hg. These corrections are as follows:

$$\eta_d = 1 - \exp(-0.0169/\sqrt{E}), \qquad (2)$$

$$t_w = 0.97, \text{ and} \qquad (3)$$

$$t_a = \exp -\ell(3.51 \times 10^{-4} + 1.76 \times 10^{-5}/\sqrt{E}) \qquad (4)$$

where E is in eV and ℓ is the air flight path in cm.

The corrected neutron spectrum with no filters, with a Cd filter, and difference between the two spectra are shown in Fig. 13. This latter (sub-cadmium) spectrum will be used to obtain an average cross section for converting foil activation measurements into an absolute average sub-cadmium neutron beam flux. Note that there is a larger fraction of neutrons in the 0.1 - 2.0 eV energy interval compared to Maxwellian and 1/E distributions as found in reactors.[11] The corrected neutron spectra with no filter and with a B_4C filter are compared in Fig. 14.

The spectral distribution of neutrons emitted from a finite hydrogenous moderator may be characterized by an epithermal component given by

$$\varphi(E) = \frac{\varphi_{epi}}{E^{\gamma}} \qquad (5)$$

where $\varphi(E)$ is the differential neutron flux (n/p·eV·sr), φ_{epi} is a constant, and the departure of γ from unity is indicative of neutron leakage. The thermal neutron differential flux can be represented by a Maxwellian-type distribution given by

$$\varphi(E) = \varphi_m \frac{E}{T^2} \exp(-E/T) \qquad (6)$$

where φ_m is the integrated Maxwellian intensity, and T is the neutron temperature in energy units. The characterization of the neutron

spectrum (in between the epithermal and thermal regions) can be completed by introducing a joining function $\Delta(E)$ given by [12]

$$\varphi(E) = \varphi_m \frac{E}{T^2} \exp(E/T) + \Delta(E) \frac{\varphi_{epi}}{E^{\gamma}}. \qquad (7)$$

An example of such a function is

$$\Delta(E) = \left[1 + \exp\left(\frac{W_1}{\sqrt{E}} - W_2\right)\right]^{-1}, \qquad (8)$$

which switches on at an energy-

$$E' = \left[\frac{W_1}{W_2}\right]^2, \qquad (9)$$

and W_2 is a measure of the spread of the switch function.

We analyze our data in the following manner:

- The slowing down neutron spectrum is characterized by fitting the data to Eq. (5) using φ_{epi} and γ as parameters.
- The Maxwellian is characterized by fitting the data to Eq. (6) using φ_m and T as parameters.
- With φ_{epi}, γ, φ_m, and T fixed, the parameters W_1 and W_2 are used to fit Eq. (7).

Both the individual fits (dashed lines) and the overall fit (solid lines) are illustrated in Fig. 15. The open circles indicate the limits of the fitting regions for the Maxwellian and slowing down portions of the spectra.

RESULTS AND DISCUSSION

We have used the spectral characterization just described to evaluate the performance of the WNR reflected 'T'-shape premoderator/moderator. We present here preliminary experimental results which are relevant to all pulsed spallation neutron sources. Our studies include the effects on moderator neutronics of varying the following: a) reflector size, b) reflector material, c) thickness and type of poison between the premoderator and moderator, and d) moderator thickness.

The neutronic performance of an unreflected 'T'-shape premoderator/moderator (see Fig. 6.) was also measured. We observed an increase of 3.9 in thermal neutron production and an enhancement of 3.5

in the slowing down region when the 'T' was surrounded by a beryllium reflector (an 'effective' cube with a side of ~45 cm). These data are shown in Fig. 16. The reflector was decoupled from the moderator by a 0.076-cm-thick Cd poison (see Fig. 8).

For a moderating reflector like beryllium and a decoupled moderator, Monte Carlo studies show that thermal neutron beam intensities quickly saturate with increasing reflector size. Neutrons scattered deep in the reflector are thermalized by the beryllium and absorbed in the decoupler; they cannot contribute to an increase in neutronic performance. For neutrons decoupled at 0.5 eV, saturation is expected to occur for a reflector radius of ~30 cm.[9] For a reflector dimensions of ~45 cm on a side comapred to ~61 cm, our data show an increase in thermal neutron beam intensity of ~15% (see Fig. 16); this is consistent with the Monte Carlo predictions.

Beryllium is the traditional candidate for a spallation neutron source reflector; we will investigate the neutronic performance of other reflector materials. We will refer to moderating reflectors like beryllium, water, etc. as 'slow' reflectors; we will call non-moderating reflectors such as copper, lead, etc., 'fast' reflectors. In future studies, we will investigate the necessary decoupling energy for 'slow' reflectors and the need for decoupling 'fast' reflectors; we will also compare the neutronic performance of different reflector materials.

In Fig. 17, we show neutron spectral comparisons from a standard moderator configuration surrounded by (decoupled) beryllium, (undecoupled) polyethylene, and (decoupled) lead/beryllium reflectors. The beryllium reflector produces a slowing-down flux ~2.3 times that for a polyethylene reflector; in the thermal region, the beryllium reflector outperforms the hydrogenous reflector by at least a factor of 2. These results are consistent with Monte Carlo studies.[13,14] The computations also show that for all decoupler energies of interest ($\lesssim$50 eV), a beryllium reflector outperforms a polyethylene reflector. The data in Fig. 17 for the lead/beryllium reflector compared to the beryllium reflector show a performance drop of ~12%. The improvised lead/beryllium reflector consisted of lead bricks crudely surrounding the premoderator (see Fig. 8) placed on a beryllium base. Computations and experiments not only indicate comparable neutronic performance between lead and beryllium reflectors, but the time-structure of neutron pulses with the lead reflector may be marginally superior.[14,15]

Data sets comparing cadmium and gadolinium poisons are shown in Fig. 18. Above ~1 eV, the effects of both poisons are similar; below ~0.2 eV, an enhancement of ~1.7 in the performance of the gadolinium poison is evident.

In Figs. 19 and 20, we show the observed thermal neutron production as a function of poison thickness and moderator thickness. These data, used in conjunction with measured neutron pulse width measurements, will be used to match moderators to the requirements of the instruments for the WNR materials science program.

TIME-ANALYZER ARM

The reduction and analysis of neutron time distribution data taken with the time-analyser arm are in a preliminary stage. We note:

- Excellent signal-to-background ratios ($\sim$100:1) have been achieved allowing orders up to (0 0 24) from PG to be clearly seen (see Fig. 21).
- Subtle differences in line shape between moderator configurations are clearly seen (see Fig. 22 and 23).

Exploitation of the capability to measure neutron pulse widths (in conjunction with neutron beam fluxes and spectra) will form a major part of our future efforts.

FUTURE PLANS

Combined neutron spectral and pulse width measurements will be used for continued optimization of the WNR spallation neutron sources. Our experimental and computational program will include:

- premoderator optimization,
- moderator-reflector and target-reflector decoupling studies,
- target material and size optimization,
- target-moderator-reflector coupling studies,
- reflector material investigations,
- cold moderator studies, and
- implementation of capability to study neutron beam quality.

ACKNOWLEDGEMENTS

This work was performed under the auspices of the U. S. Department of Energy. We acknowledge the support and encouragement of R. Woods, and useful discussions with J. M. Carpenter. We appreciate the help of J. R. Baldonado and K. J. Hughes in setting up the experiments, and E. R. Whitaker in the experiment design. We acknowledge the cooperation of the WNR operations crew of R. D. Ryder (head), H. M. Howard, R. A. Johnson, and M. R. Lopez.

REFERENCES

1. G. J. Russell, et al., "The WNR Facility--A Pulsed Spallation Neutron Source at the Los Alamos Scientific Laboratory," Intl. Conf. on Neutron Physics and Nucl. Data for Reactors and Other Applied Purposes, Harwell, England (1978).

2. M. S. Livingston, "LAMPF a Nuclear Research Facility," Los Alamos Scientific Laboratory report LA-6878-MS, UC-28 and UC-34 (September 1977).

3. G. J. Russell, et al., "Spallation Target-Moderator-Reflector Studies at the Weapons Neutron Research Facility," Symp. on Neutron Cross Sections from 10-50 MeV, Brookhaven National Laboratory, Upton, NY, May 12-14, 1980, BNL-NCS-51245, Vol. I, pp. 169-192.

4. G. J. Russell, et al., "Measurements of Spallation Target-Moderator Reflector Neutronics at the Weapons Neutron Research Facility," Proc. of the 4th Meeting of the International Collaboration on Advanced Neutron Sources (ICANS-IV), National Laboratory for High Energy Physics (KEK), Tsukuba, Japan, October 20-24, 1980, KENS report II (March 1981).

5. T. W. Armstrong and K. C. Chandler, "Operating Instructions for the High Energy Nucleon Meson Transport Code HETC," Oak Ridge National Laboratory report ORNL-4744 (January 1972).

6. Los Alamos Monte Carlo Group, "MCNP--A General Monte Carlo Code for Neutron and Photon Transport, Version 2B," Los Alamos National Laboratory report LA-7396-M, Revised (April 1981).

7. H. Kschwendt and H. Rief, "TIMOC--A General Purpose Monte Carlo Code for Stationary and Time Dependent Neutron Transport," Euration report EUR 4915e (1970).

8. D. Picton, Ph. D. Thesis, University of Birmingham, U. K. (1981).

9. A. D. Taylor, "Neutron Transport from Targets to Moderators," Proc. of Meeting on Targets for Neutron Beam Spallation Sources, Jül-Conf-34. ISSN 0344-5798 Jülich (1980).

10. V. Agoritsas and R. L. Witkover, "Tests of SEC Stability in High Flux Proton Beams," IEEE Trans. on Nucl. Science, Vol. NS-26. No. 3, pp. 3355-3356 (1979).

11. J. M. Carpenter, et al., "IPNS--A National Facility for Condensed Matter Research," Argonne National Laboratory report ANL-78-88 (November 1978).

12. K. H. Beckurts and K. Wirtz, Neutron Physics, (Springer-Verlag, New York Inc., 1964) Ch. 10.

13. G. J. Russell, Los Alamos Scientific Laboratory, unpublished data, December 1973.

14. A. D. Taylor, "Monte Carlo Reflector Studies for a Pulsed Spallation Source," these proceedings.

15. G. S. Bauer, et al., "Measurement of Time Structure and Thermal Neutron Spectra for Various Target-Moderator-Reflector Configurations of an Intensity-Modulated Spallation Neutron Source," Realisierungsstudie zur Spallations-Neutronenquelle, Teil II (to be published.)

TABLE I
PROGRAM FOR MEASURING SPALLATION TARGET-MODERATOR-REFLECTOR NEUTRONICS AT THE WEAPONS NEUTRON RESEARCH FACILITY

GENERAL GOALS

- Obtain basic data relevant to spallation neutron source development, accelerator breeder technology, and computer code validation
- 'Optimize' a target-moderator-reflector configuration for materials science research at the present WNR and any upgraded WNR
- Characterize WNR targets and moderators for nuclear physics applications

SPECIFIC OBJECTIVES

- Measure the effects of different targets, moderators, reflectors, and decouplers on thermal and epithermal neutron beam fluxes and thermal neutron pulse widths
- Ascertain the 'practical' gain of a uranium spallation target (versus lead, tantalum, tungsten, etc.) by measuring thermal neutron beam fluxes and pulse widths
- Measure the high-energy neutron and particle contamination in thermal neutron beams for offset and center-looking geometry
- Study neutron yields and pulse widths from cold moderators
- Measure neutron production and spectra from thin and thick targets
- Measure the fertile-to-fissile conversion yields inside thick targets of thorium and depleted uranium
- Measure energy deposition in spallation targets and cold moderators
- Compare all measurements with calculated predictions

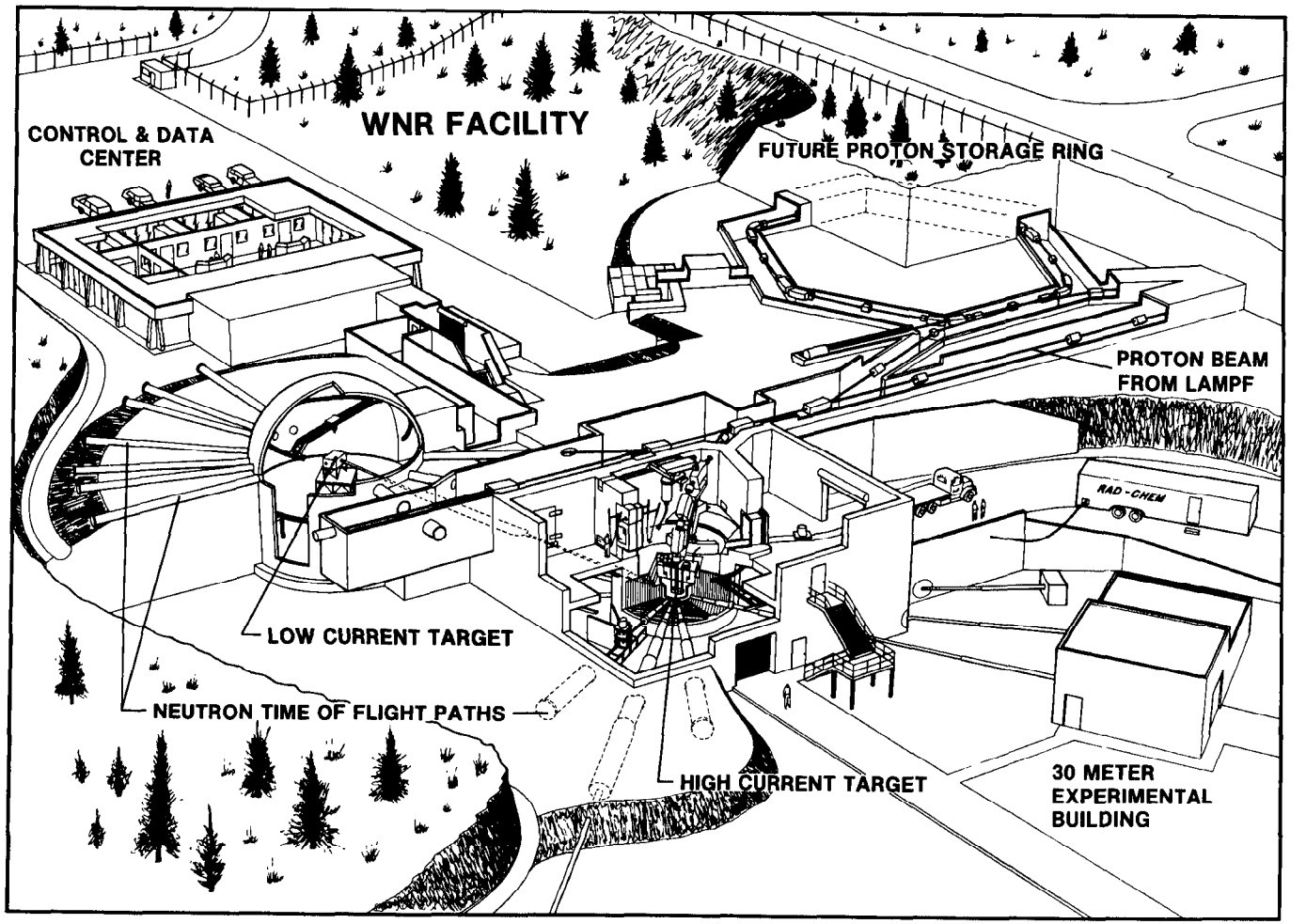

Fig. 1. General layout of the WNR showing the two target areas. The high-current target is located in a vertical proton beam and is viewed by 11 horizontal flight paths. The low-current target is located in a horizontal proton beam and viewed by 11 horizontal flight paths and one vertical flight path.

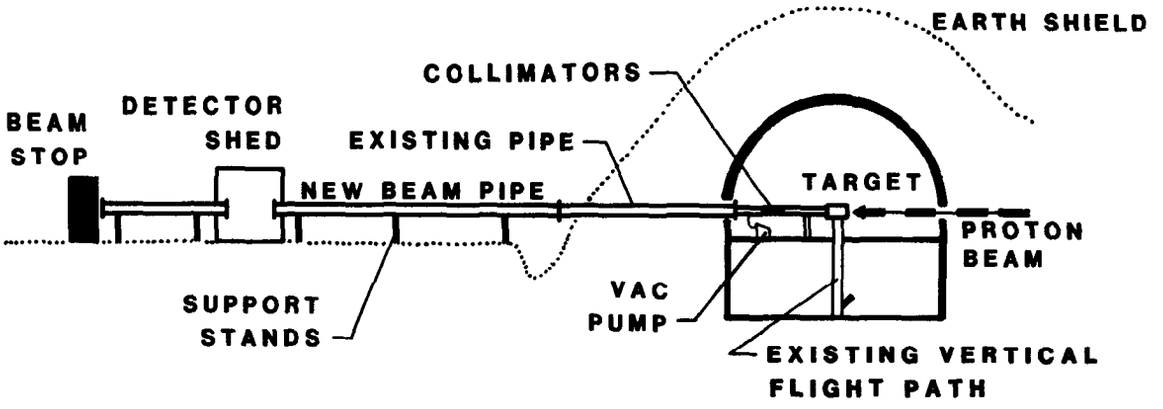

Fig. 2. Section through the low-current target area showing the location of the vertical flight path.

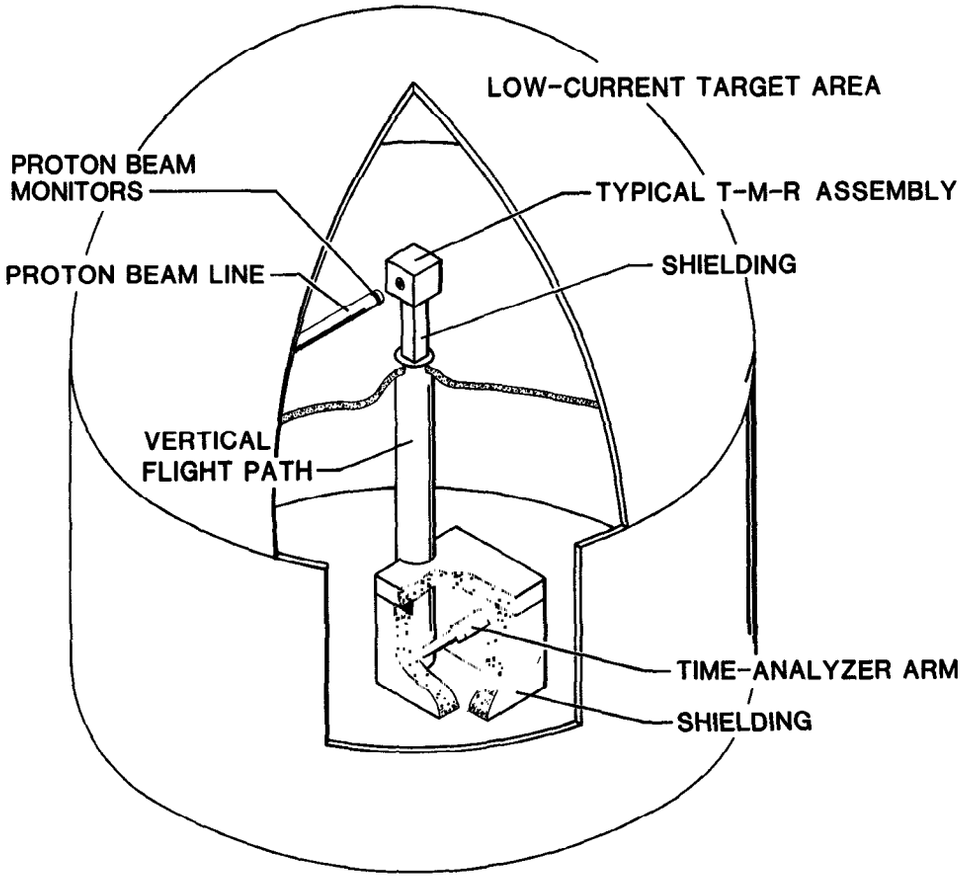

Fig. 3. Location of a target-moderator-reflector assembly, the vertical flight path, and the time analyzer arm in the low-current target area.

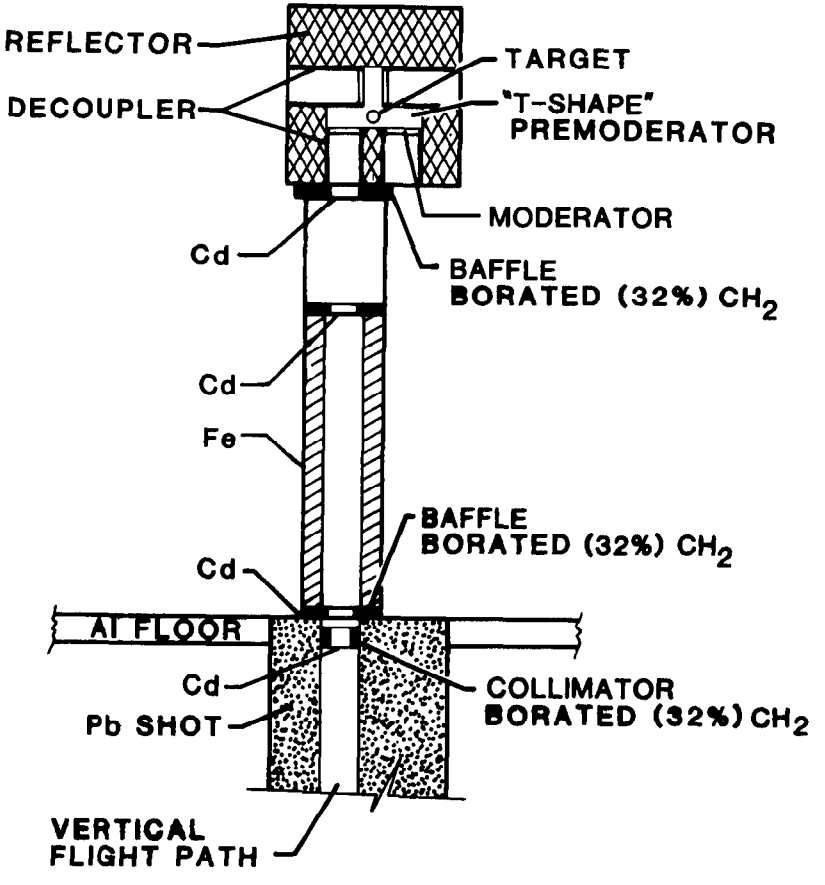

Fig. 4. Detail of the upper portion of the vertical flight path.

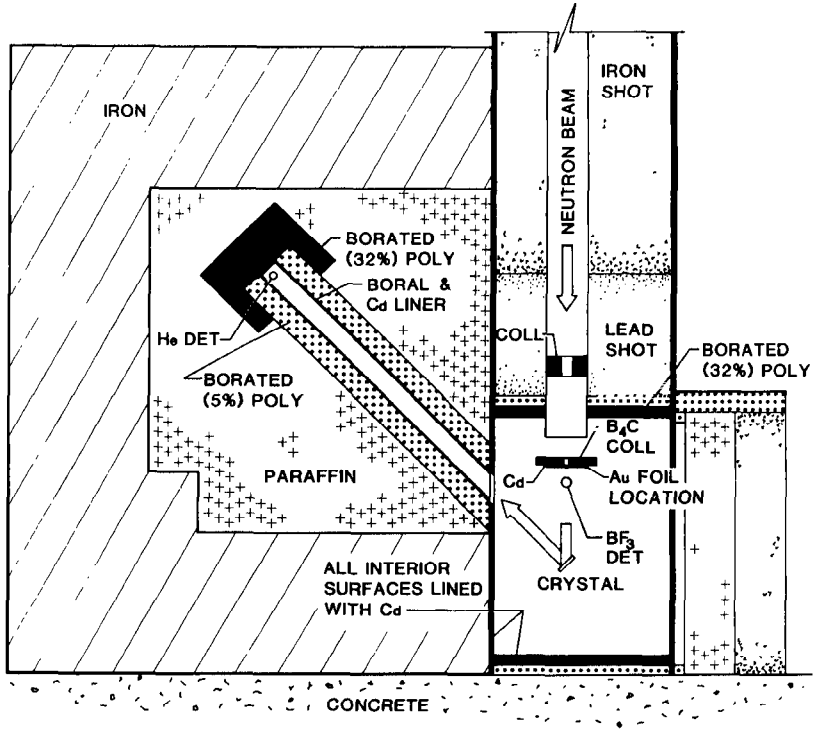

Fig. 5. Detail of the time analyzer arm and location of the BF_3 detector at the bottom of the vertical flight path.

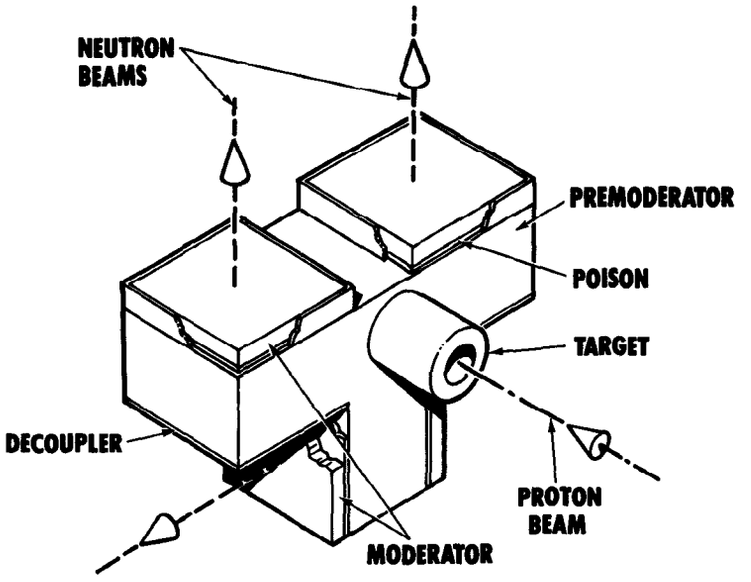

Fig. 6. Unreflected 'T'-shape premoderator/moderator.

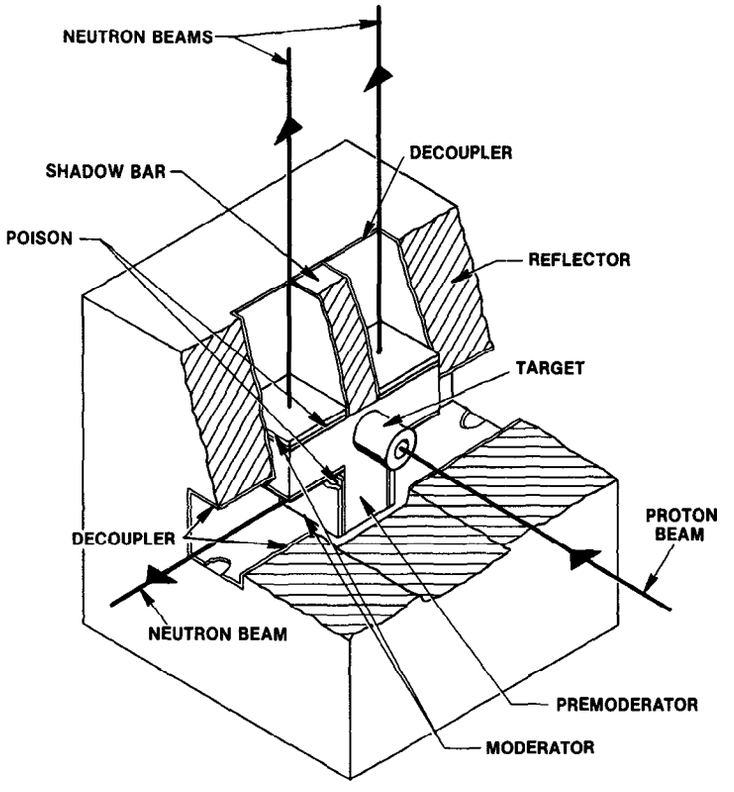

Fig. 7. Reflected 'T'-shape premoderator/moderator.

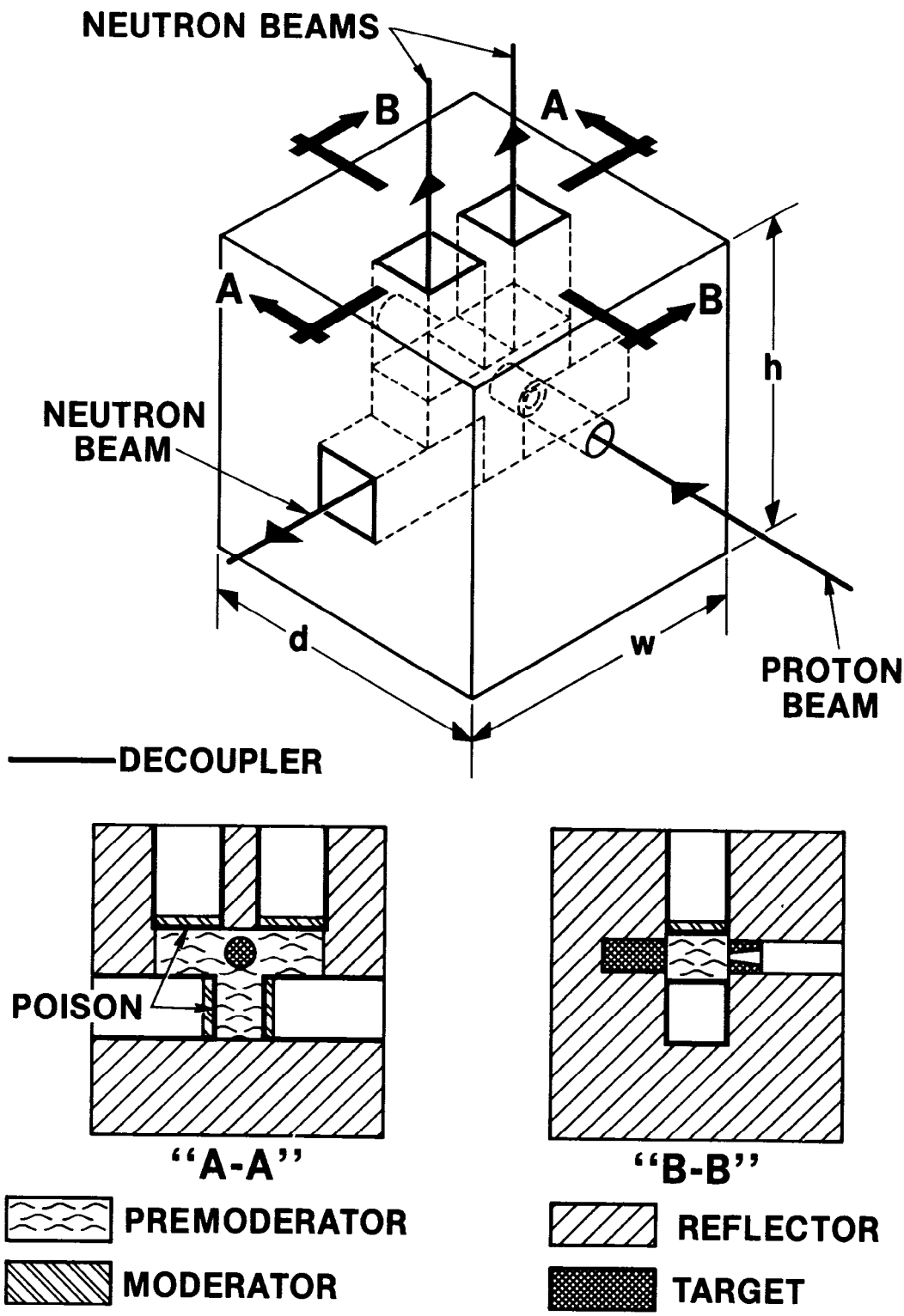

Fig. 8. Section thru a reflected 'T'-shape premoderator/moderator.

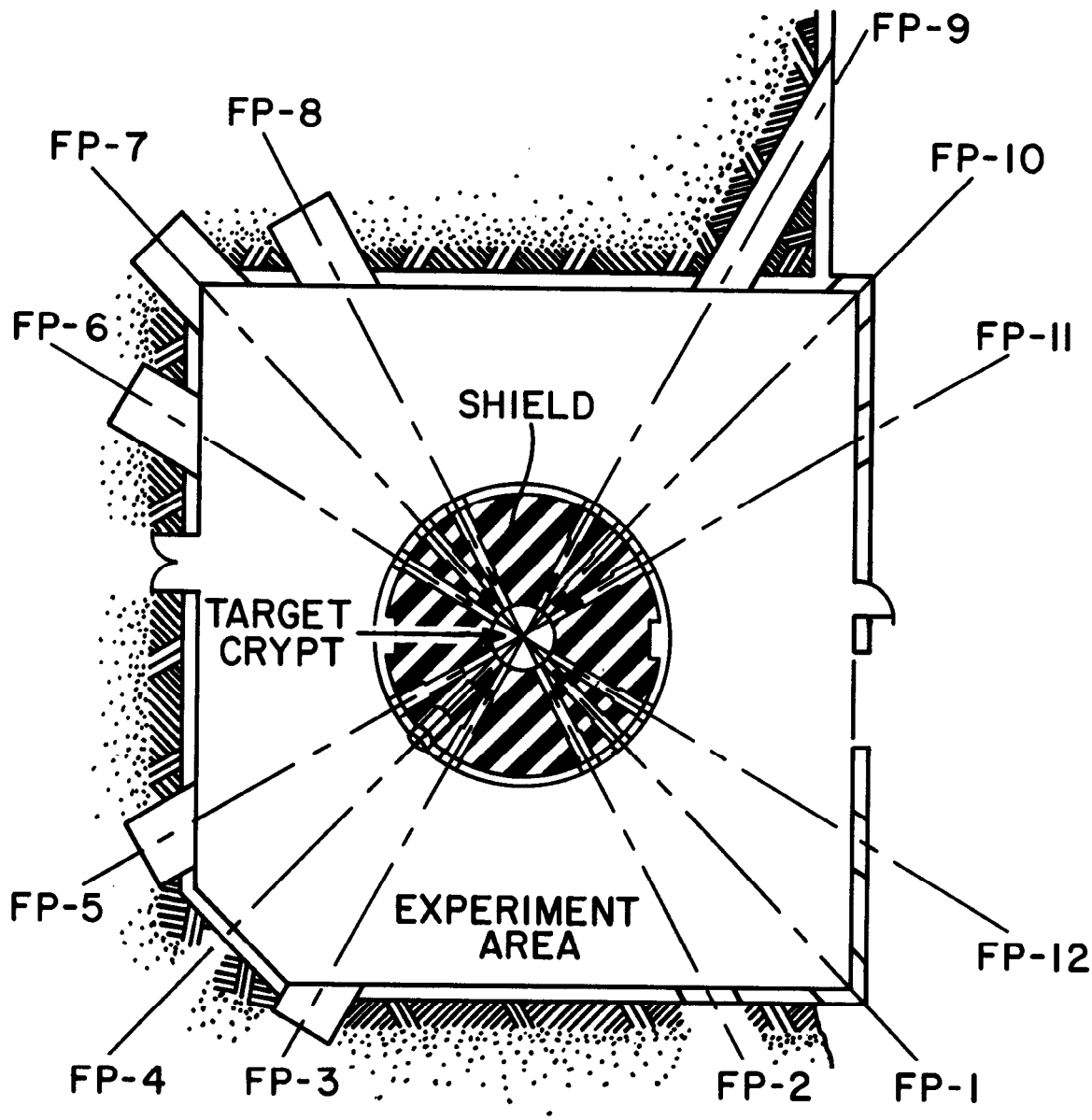

Fig. 9. Layout of the neutron flight paths in the WNR high-current target area.

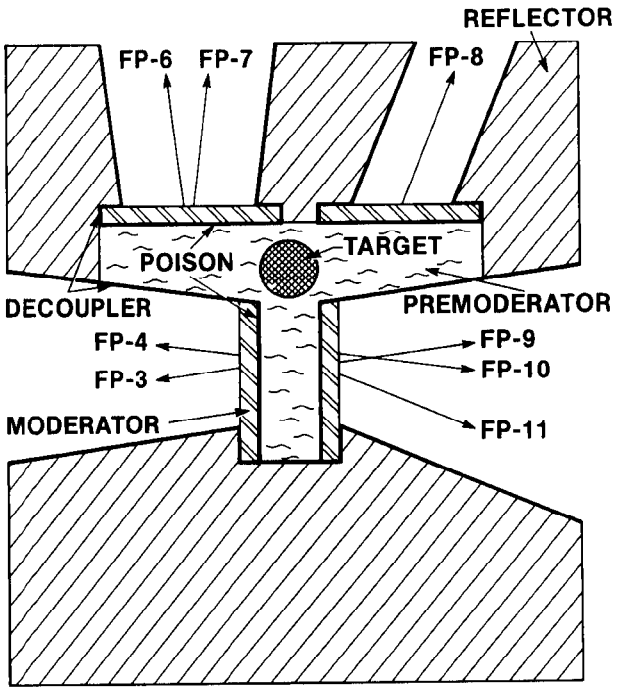

Fig. 10. Section through a reflected 'T'-shape premoderator/moderator configuration showing the location of various neutron flight paths (in the WNR high-current target area) relative to moderator surfaces.

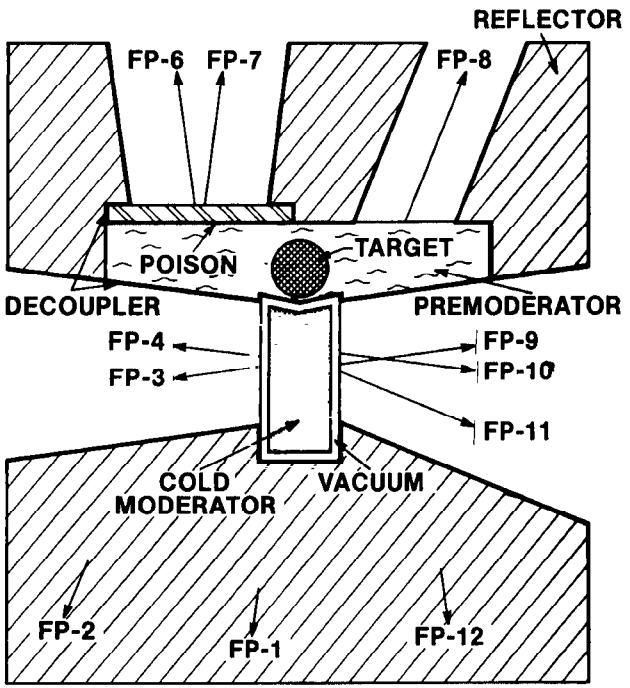

Fig. 11. A possible reflected 'T'-shape premoderator/moderator configuration in which the various moderators are 'optimized' for each cluster of flight paths in the WNR high-current target area.

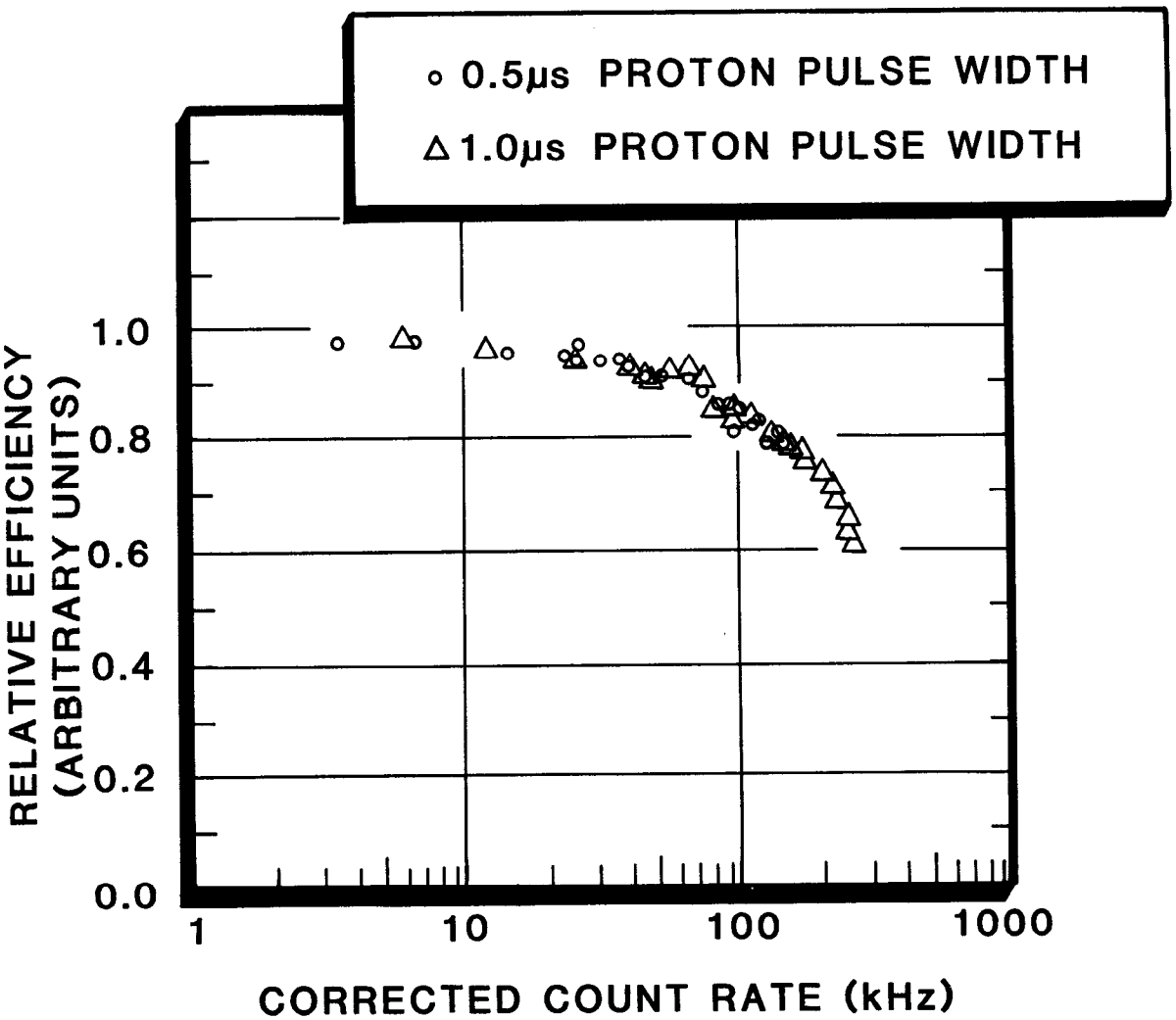

Fig. 12. Count rate dependence of BF_3 detector response.

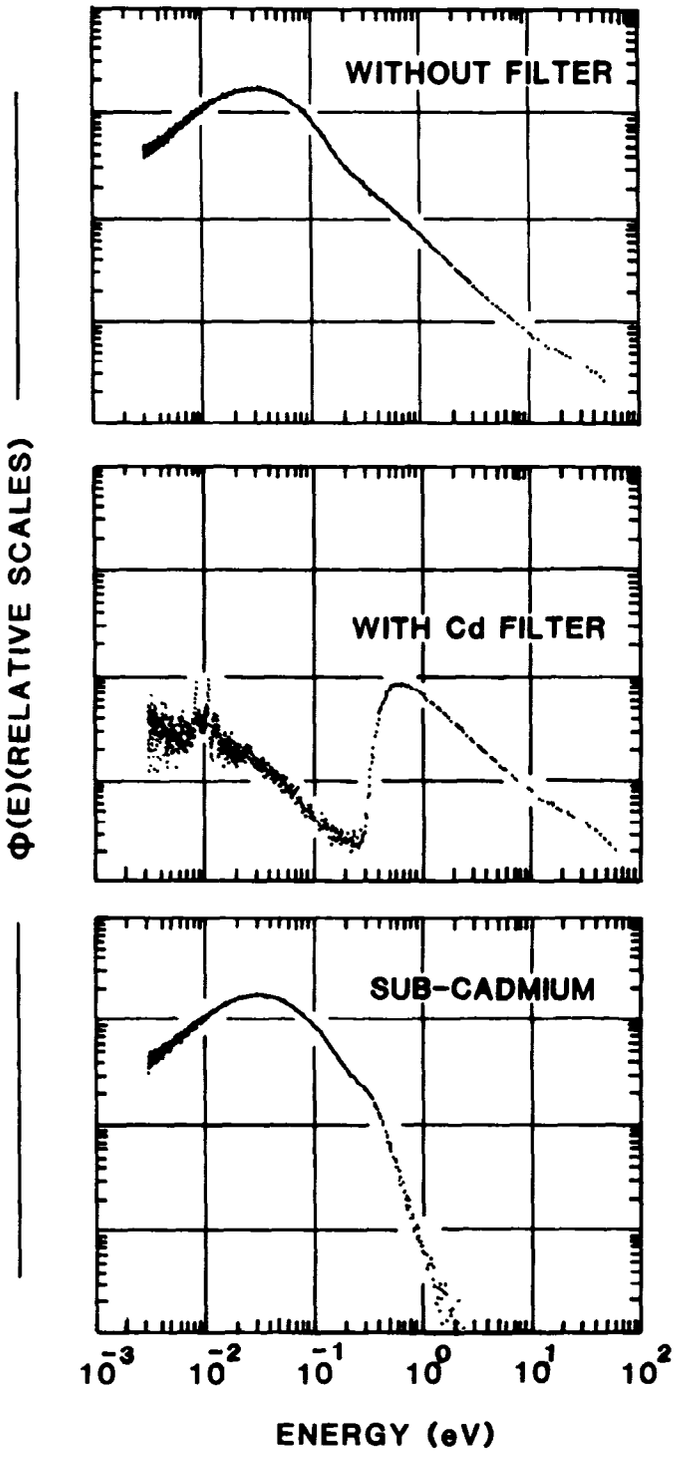

Fig. 13. Measured neutron spectra with and without a cadmium filter. The difference between these two spectra gives the sub-cadmium neutron spectrum.

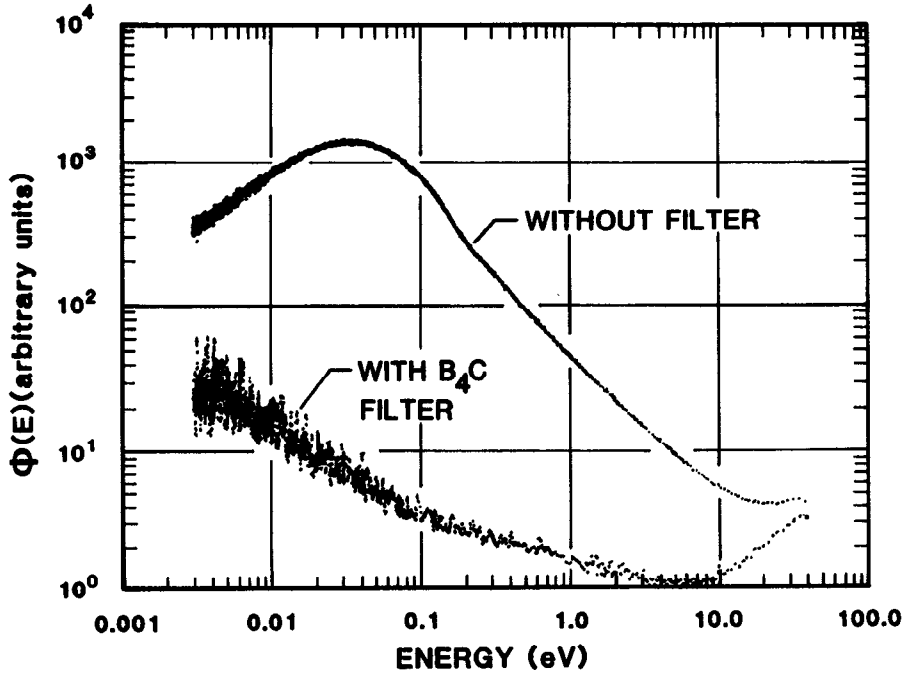

Fig. 14. Measured neutron spectra with and without a B_4C filter.

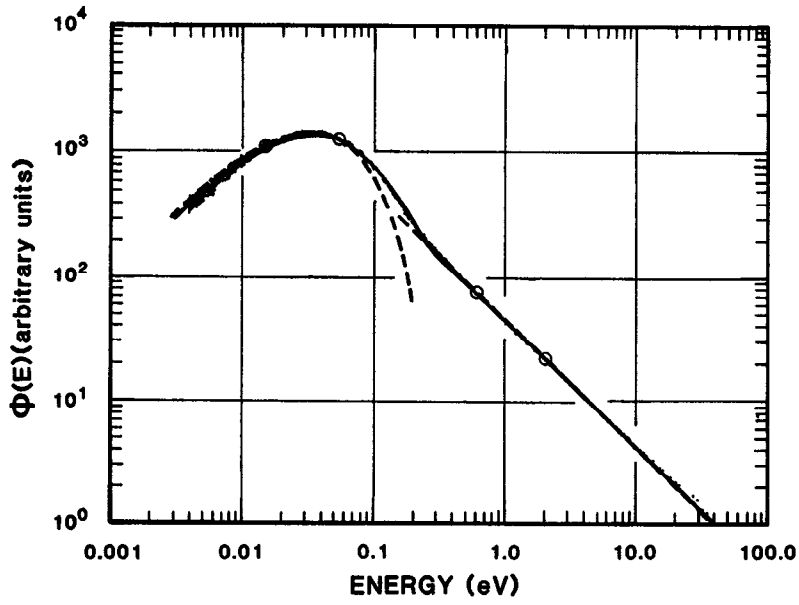

Fig. 15. A fit of Eq. 7 in the text to a representative data set. The dashed lines are independent fits to the Maxwellian and slowing down portions of the spectrum. The solid curve is the overall six parameter fit using a joining function.

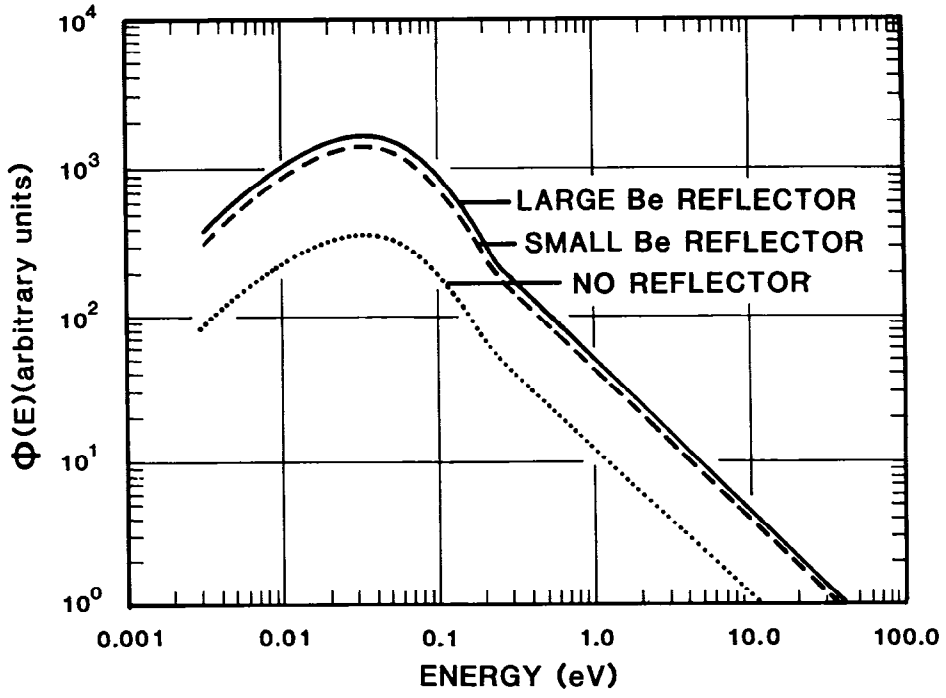

Fig. 16. Measured neutron spectra using a large and small beryllium reflector. The measured neutron spectrum from a unreflected system is also shown.

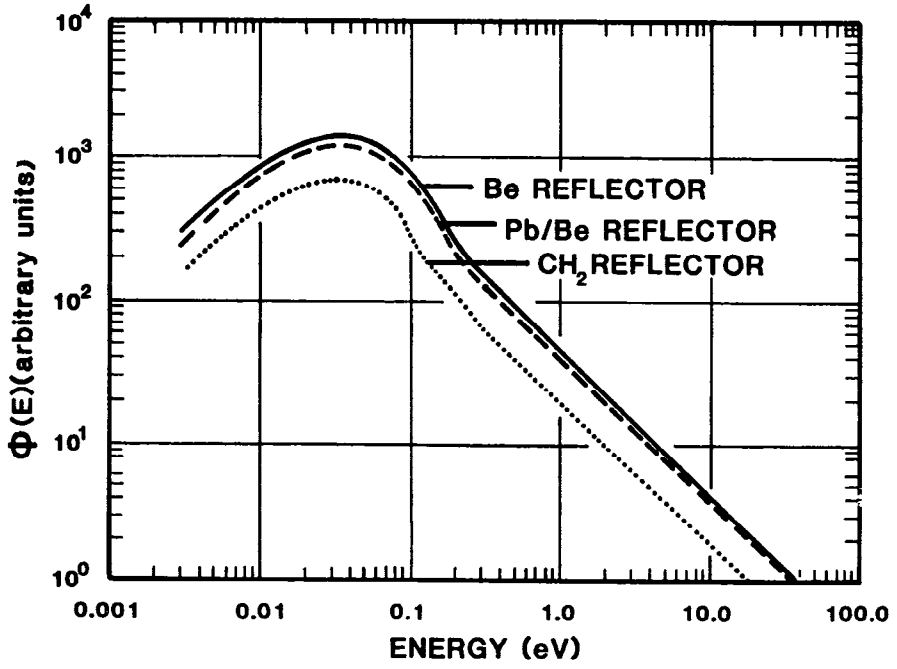

Fig. 17. Measured neutron spectra using beryllium, polyethylene, and beryllium-lead reflectors.

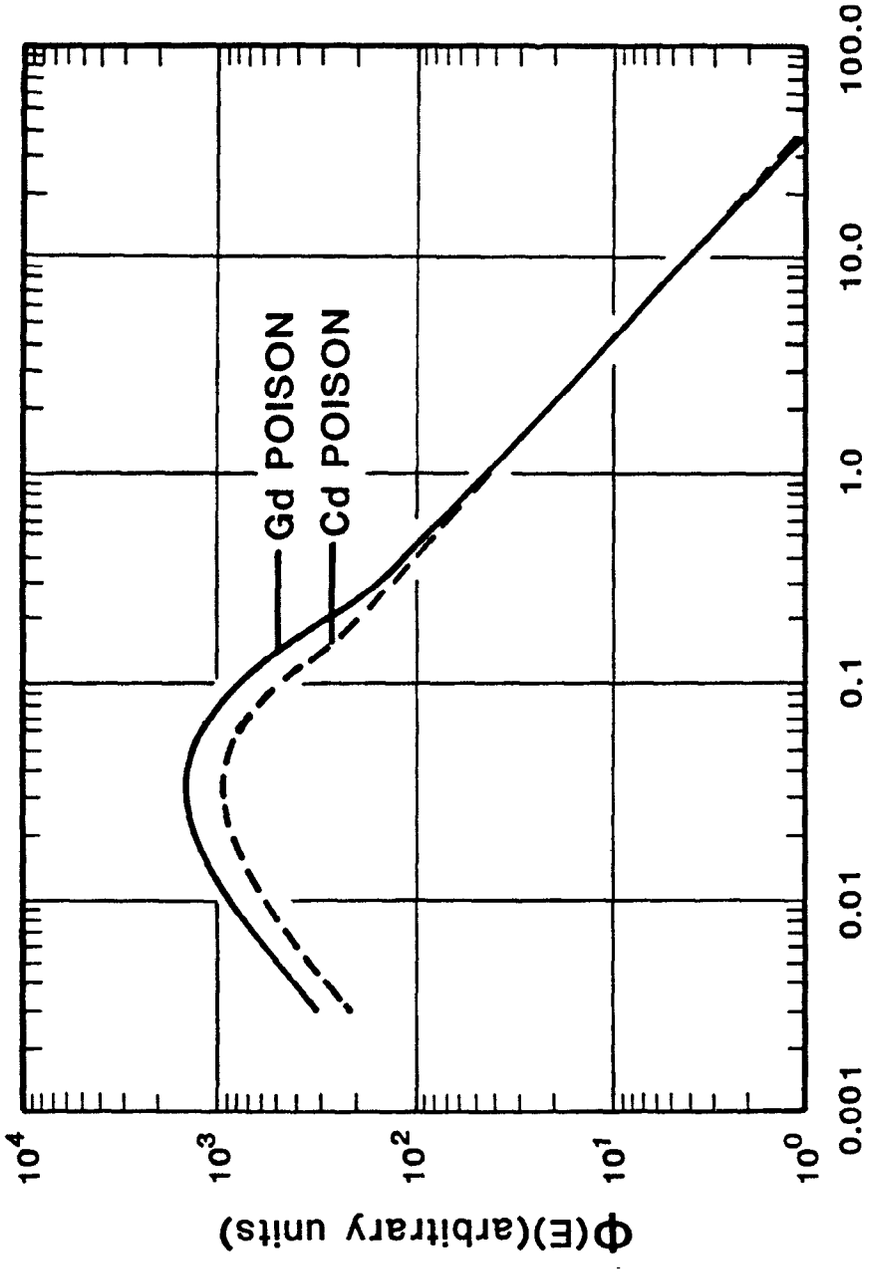

Fig. 18. Measured neutron spectra from a moderator poisoned at a depth of 1.27 cm by gadolinium and cadmium. The gadolinium was 0.0025-cm thick, and the cadmium was 0.076-cm thick.

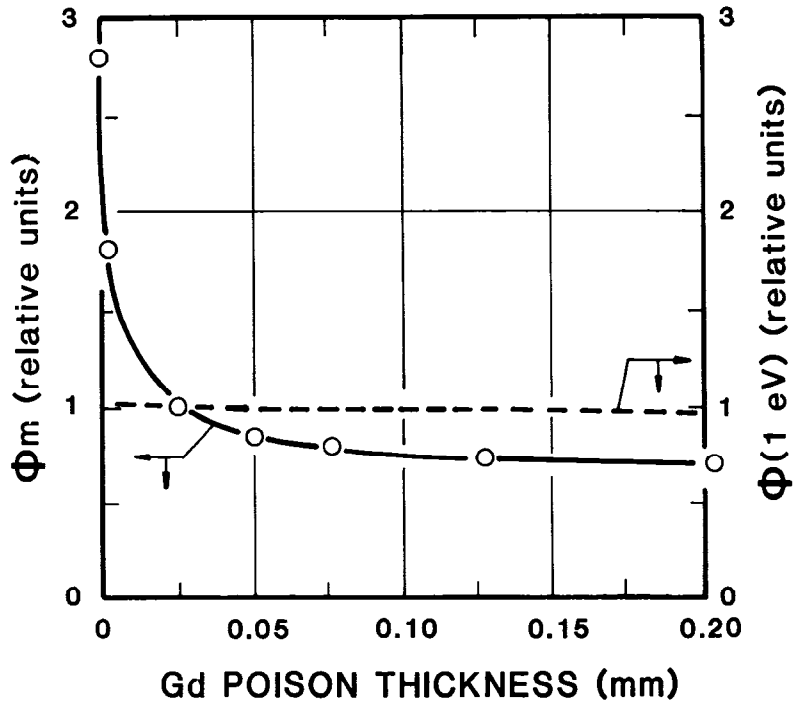

Fig. 19. Variation of measured thermal and 1-eV neutron fluxes from a moderator as a function of gadolinium poison thickness.

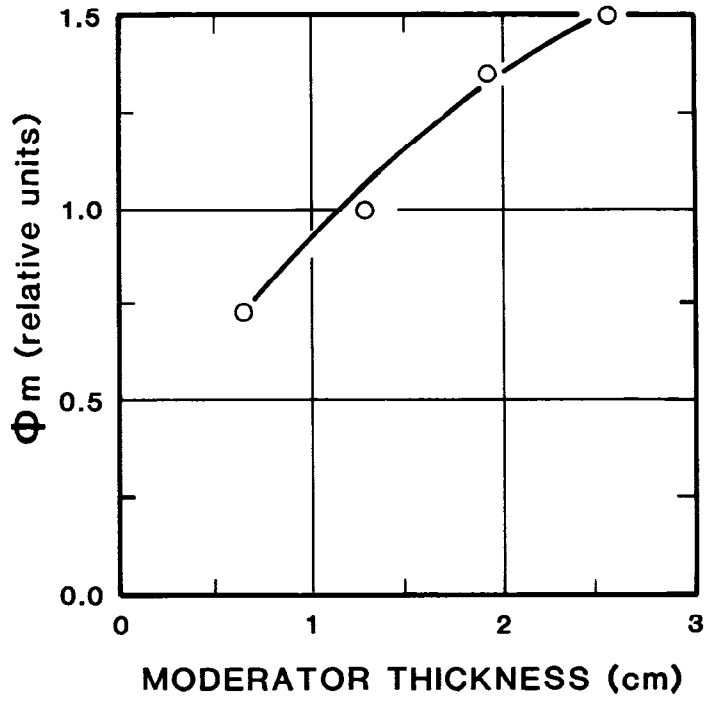

Fig. 20. Variation of measured thermal neutron flux from a moderator as a function of moderator thickness.

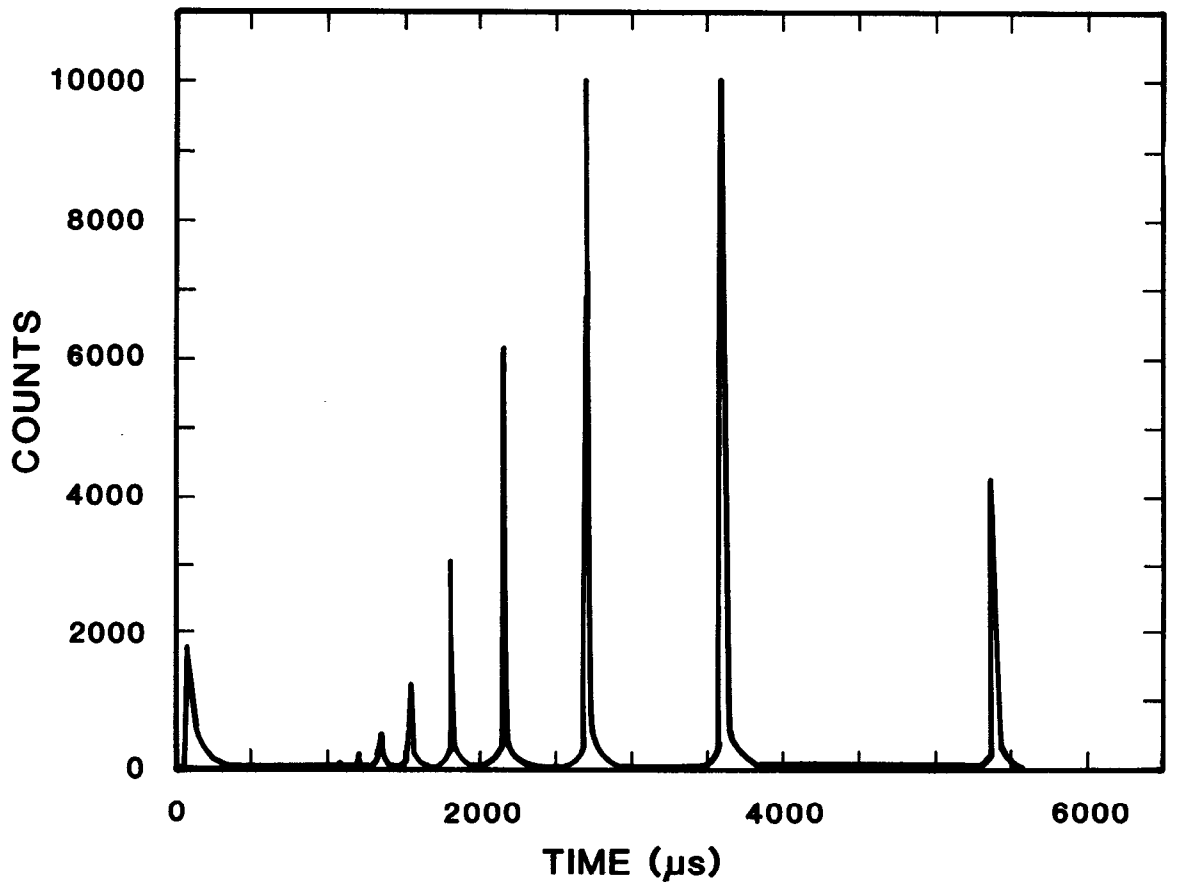

Fig. 21. Time distribution of neutrons diffracted by the (0 0 2ℓ) planes of pyrolitic graphite, starting with the (0 0 4) reflection.

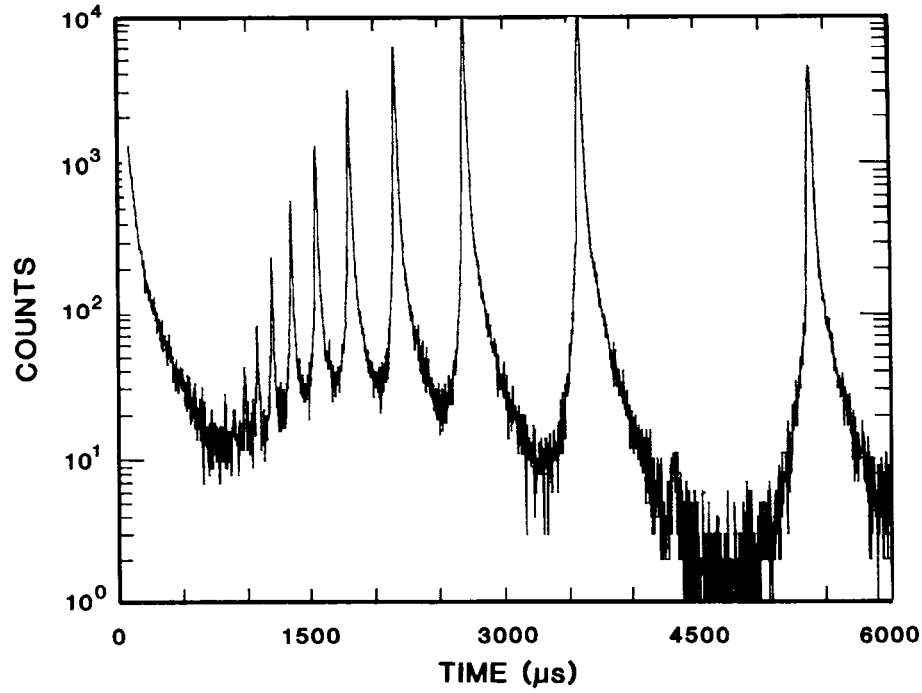

Fig. 22. Semi-log plot of measured neutron time distributions from a gadolinium poisoned moderator.

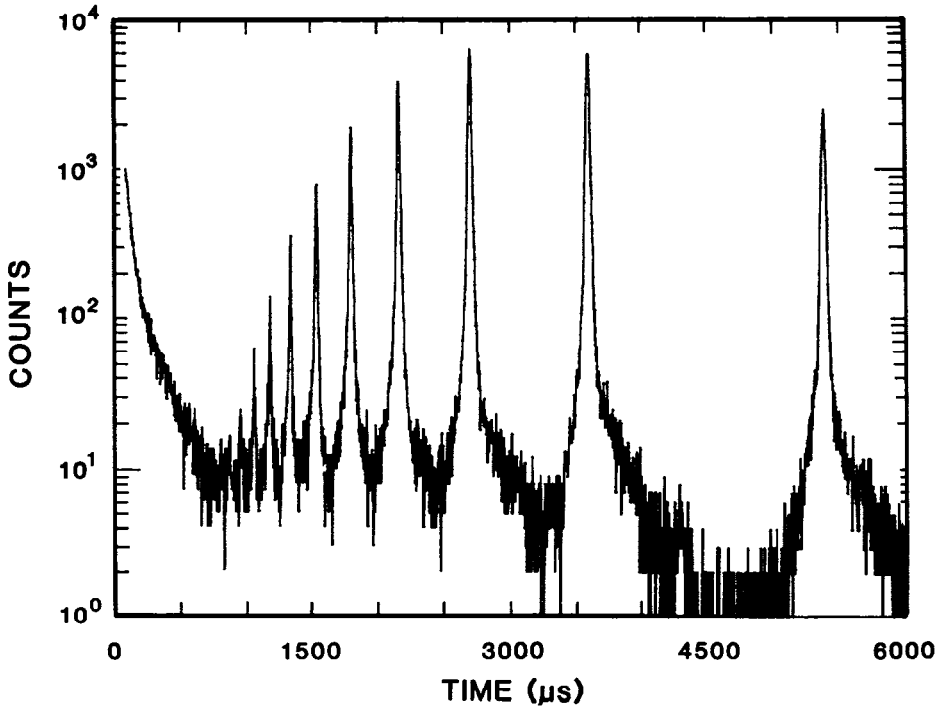

Fig. 23. Semi-log plot of measured neutron time distributions from a cadmium poisoned moderator.